Synergistic effect of animal oil or butter and hydrogen peroxide on physical and mechanical properties of porous alumino-siliceous materials

Narumon Lertcumfu[a], **Kannikar Kaewapai**[a,b], **Pharatree Jaita**[a,c], **Ratabongkot Sanjoom**[d], **Gobwute Rujijanagul**[a,c,e,f,*], **Tawee Tunkasiri**[a,c]

[a] Department of Physics and Materials Science, Faculty of Science, Chiang Mai University, Chiang Mai 50200 Thailand
[b] Graduate School, Chiang Mai University, Chiang Mai 50200 Thailand
[c] Science and Technology Research Institute, Chiang Mai University, Chiang Mai 50200 Thailand
[d] Department of Applied Science and Biotechnology, Faculty of Agro-Industrial Technology, Rajamangala University of Technology Tawan-ok Chantaburi Campus, Chantaburi 22210 Thailand
[e] Materials Science Research Center, Faculty of Science, Chiang Mai University, Chiang Mai, Thailand
[f] Research Center in Physics and Astronomy, Faculty of Science, Chiang Mai University, Chiang Mai 50200 Thailand

*Corresponding author, e-mail: rujijanagul@yahoo.com

ABSTRACT: Porous alumino-siliceous (PAS) materials are attractive for use in a wide variety of construction and adsorption materials. In the present study, the porous alumino-siliceous materials were synthesized by a geopolymerization method in a reaction from ceramic waste, metakaolin, and an alkaline solution, H_2O_2 (as a foaming agent) and either pork lard or butter (surfactants). Different amounts of the surfactants (2.5–15 wt%) were added to the samples. The pore shape in the PAS materials was affected by the type of surfactant used. PAS materials with small open pores and high porosity were successfully fabricated with butter as a surfactant. The compressive strength value trend was related to total porosity. The relationship between compressive strength and porosity was found to be consistent with a model proposed by Ryshkewitch. The results suggest that this material can be used as a foam material.

INTRODUCTION

Alumino-siliceous materials are pozzolanic materials containing reactive silica and alumina [1]. Pozzolanic materials are well known as construction materials, wastes, and ashes produced from some agricultural materials, e.g., metakaolin, calcined clays, fly ash, slag, rice husk, sawdust, palm kernel shells, and sugarcane bagasse [1–3]. Pozzolanic materials have been used as precursors for geopolymer materials, which are obtained by the reaction of aluminosilicates with a highly alkaline environment, leading to the formation of a continuous three-dimensional network of inorganic molecules linked by covalent bonds [4]. These structures are composed of one tetrahedral silicate and aluminate units that are connected to each other by sharing one common oxygen atom [4–6]. Geopolymer materials is one of the most promising alternative materials, which was first discovered by Davidovits [7]. Geopolymer materials are attractive because of their good chemical resistance, high-temperature resistance, high early strength, high durability, thermal stability, low shrinkage, lightweight, low cost, and environmental friendliness [8–13]. All of the advantageous properties of geopolymer materials make them very interesting materials for forming geopolymer foams.

Geopolymer foams (porous alumino-siliceous materials, PAS) are lightweight materials consisting of geopolymer paste with a high degree of a homogeneous void, or pore structure, inside the materials due to small air bubbles having been introduced to the geopolymer matrix. Controlling the pore structure (i.e., shape, morphology, and size), total porosity, and pore size distribution are important parameters for generating geopolymer foams, for which the voids and pores determine the density

and strength [14–16]. PAS materials have been applied in many applications such as for photocatalytic degradation, membranes, high-efficiency adsorption materials, and building materials [16, 17].

To fabricate the foam, pore foaming agents such as silicon [18] metallic aluminum powder [19], and H_2O_2 [16–19] are used to produce the air bubbles in geopolymer foams. However, these pore foaming agents often create closed pores which reduce the total surface area of the sample. This can make them unsuitable for some applications. To solve this problem, stabilizing agents such as surfactants, fibers, and particles can be used for addition into the geopolymer slurry to decrease the surface tension of the gas/slurry system [20, 21]. Surfactants such as Triton X 100 [22], Tween 80 [21], protein [23], and vegetable oil [16, 24] are classified in the hydrophilic group and are used for this purpose. One of the interesting surfactants is oil due to its lower cost than the pure chemical of surfactants, and the result from previous researches [16, 24] reported that the reaction between high alkaline geopolymer and fatty acid in oils via a saponification reaction can create the interconnect porous [25]. Typical properties of the fatty acid collected from the literature are given in Table 1. A typical representation of fatty acid compositions is $C_{x:y}$ in which x is the number of carbons, y is the number of double bonds. Generally, $C_{16:0}$ (Palmitic acid) is the most common saturated fatty acid in animals, plants, and microorganisms, and $C_{18:1}$ (Oleic acid) is the most common monounsaturated fatty acid in plants, animals and microorganisms [26].

Recently, the properties of geopolymer foams that contain vegetable oil as a surfactant and H_2O_2 as a foaming agent have been reported [16, 24]. It has been proposed that the type of vegetable oil slightly affected the total porosity, average pore size, and pore size distribution, but significantly affected the compressive strength of the samples. In the present work, we demonstrate that animal oil or products from animals can be used as alternative surfactants. Furthermore, data for products from animals as geopolymer surfactants is lacking. Therefore in the present work, geopolymer foam was fabricated. The synergistic effects of animal oil or butter as a surfactant and hydrogen peroxide as a foaming agent were investigated. To reduce industrial waste, ceramic waste from a ceramic factory was used as a raw material in this work.

MATERIALS AND METHODS

Ceramic waste (CW, or calcined clays) from A.P.K Dewkoo (from Ang Thong province, Thailand) and kaolinite (from Ranong province, Thailand) were used as raw materials to fabricate porous alumino-siliceous materials. The ceramic waste was crushed into a fine powder by grinding, using mortar and ball milling technique. Kaolinite was calcined at 750 °C for 3 h to obtain metakaolin (MK) and then crush into a fine powder using a ball milling technique. Chemical analysis was performed with an X-ray Fluorescence (XRF) technique. To form the porous alumino-siliceous materials, a 15 M NaOH solution was prepared by dissolving sodium hydroxide (98% purity sodium hydroxide, the brand name of Praatit) with deionized water for at least 24 h at room temperature to complete the exothermic reaction. Sodium silicate (Na_2SiO_3) was purchased from World Chemical Industrial (Thailand) with the chemical composition of 16.32% Na_2O, 34.60% SiO_2 and 49.08% H_2O (mole ratio SiO_2/Na_2O = 2.19) and with a specific gravity at 20 °C of 1.54 g/cm^3. The Na_2SiO_3 solution was diluted with water (61% $Na_2SiO_3^+$ 49% H_2O) and mixed by stirring for 24 h. The NaOH and Na_2SiO_3 solution were mixed to prepare the alkaline activator solution and left to cool down to room temperature. Hydrogen peroxide (H_2O_2) was used as the foaming agent. H_2O_2 with a concentration of 30 wt% was diluted with water to 3 wt%. A 0.24 wt% solution of diluted H_2O_2 (3 wt%) was used to substitute some of Na_2SiO_3. Butter and pork lard (Unsalted butter, Orchid) was used as a surfactant, ranging from being 2.5–15 wt% of the sample. To prepare the pork lard, pork fat was heated on a cast-iron skillet, keeping the heat below the fat's smoke point until pork lard was obtained. To form the PAS samples, the ratios of the mixtures of ceramic waste/MK and Na_2SiO_3/NaOH were 1.4 and 1.14, respectively. The PAS materials were prepared in the following manner. First, ceramic waste and metakaolin were mixed together. The obtained powder was then mixed together with the alkaline solution. Butter and pork lard were heated up to 35 °C to get a liquid, and then 3 wt% of H_2O_2 with either pork lard or butter were added into the slurry. The mixture contents were mixed together until a homogeneous slurry was obtained. The slurry was then poured into a cube-shaped plastic mold (1.5 × 1.5 × 1.5 cm) which was vibrated for 5 min and cured at room temperature. Finally, the residual pork lard and butter was removed by soaking the PAS material in

Table 1 Fatty acid compositions of vegetable oil, pork lard, other animal fats, and products from live animals [26–34].

Source	Fatty acid (% w/w)										
	$C_{12:0}$	$C_{14:0}$	$C_{16:0}$	$C_{16:1}$	$C_{17:0}$	$C_{18:0}$	$C_{18:1}$	$C_{18:2}$	$C_{18:3}$	$C_{20:0}$	$C_{20:1}$
Olive oil	–	0.7	11.5	–	–	2.0	78.6	7.0	–	0.2	–
Sunflower oil	–	–	3.7	–	–	2.0	31.5	60.5	–	2.3	–
Pork lard[a]	–	1.5	25.4	2.4	–	13.3	41.4	13.4	–	–	–
Pork lard[b]	–	1.3	20.6	1.9	0.5	10.9	39.1	19.6	1.2	0.9	0.9
Beef tallow	2.0	6.0	28.0	–	–	22.0	38.0	3.0	1.0	–	–
Beef fat	–	2.9	24.5	2.8	1.3	17.8	28.6	1.8	0.8	0.1	0.2
Chicken fat	–	0.9	28.3	5.8	0.2	6.7	41.1	14.3	0.6	0.1	
Mutton fat	–	6.7	20.7	0.9	2.0	28.0	33.9	1.3	0.8	0.6	0.1
Cod liver oil	–	4.2	11.9	6.9	0.2	2.3	21.1	0.4	1.9	0.1	11.4
Butter	3.9	12.9	31.4	2.0	–	12.1	30.2	2.1	–	0.8	1.6
Margarine	0.2	1.1	48.7	0.2	–	5.0	33.9	9.8	0.4	–	–

[a] Pork lard from local commerce (São Paulo, Brazil).
[b] Pork lard from slaughtered houses in Yogyakarta (Indonesia).

hot water (80 °C), which was replaced every 20–40 min, until it cleared up.

The phase formation of the PAS samples was carried out using an X-ray diffraction technique (XRD). The XRD patterns (2θ) were measured in a range from 10–60°. The bulk density, porosity, and water absorption of each PAS sample were determined using Archimedes' method. The data presented are the averages of three replicates. The bulk density, porosity, and water absorption were calculated using the following equations:

$$\text{Bulk density} = \frac{W_d}{W_{ssd} - W_w} \times \rho_{water} \quad (1)$$

$$\text{Porosity} = \frac{W_{ssd} - W_d}{W_{ssd} - W_w} \times 100 \quad (2)$$

$$\text{Water absorption} = \frac{W_{ssd} - W_d}{W_w} \times 100 \quad (3)$$

where W_{ssd} is the specimen weight in the saturated surface dry condition (g), W_d is the specimen dry weight after 24 h in an oven (g), W_w is the weight of saturated specimen (g), ρ_{water} is the density of water (g/cm³). The total porosity (p) was calculated according to the equation:

$$p = \left(1 - \frac{\rho_b}{\rho_t}\right) \times 100 \quad (4)$$

where ρ_b is bulk density and ρ_t is true density. The microstructure of the samples was investigated with a scanning electron microscope (SEM, JEOL JSM-5910 LV). A mechanical property, i.e., the compressive strength, was tested using compression machines on at least six specimens after curing for 3 days.

Table 2 The major chemical compositions (%) of ceramic waste, kaolinite, and metakaolin.

Oxide	Ceramic waste	Kaolinite	Metakaolin
SiO_2	57.30	47.87	55.64
Al_2O_3	12.80	36.66	38.60
Fe_2O_3	17.94	0.05	0.70

RESULTS AND DISCUSSION

The chemical compositions of ceramic waste, kaolinite, and metakaolin were analyzed with an X-ray Fluorescence (XRF) technique. The chemical compositions of the ceramic waste, kaolinite, and metakaolin consisted of many components, e.g., Al_2O_3, SiO_2, Fe_2O_3, K_2O, MgO, Na_2O, and TiO_2. However, the major components of these materials were Al_2O_3, SiO_2, Fe_2O_3, as shown in Table 2. The XRD patterns of PAS materials are shown in Fig. 1. The XRD result revealed that the samples contained a multiphase, including a major phase of quartz and minor phases of rutile (TiO_2) and hematite (Fe_2O_3). This result corresponded with the XRF result.

Fig. 2(a–d) and Fig. 3(a–d) show the prototype precasts of PAS samples produced using H_2O_2 as a foaming agent, and respectively containing butter or pork lard as different surfactants used in varying amounts. Orange-brown color of the samples was caused by the ceramic waste powders (raw material) containing Fe_2O_3. The PAS samples containing butter had higher porosity at the surface, than that of the PAS samples with pork lard. However, the surface porosity was found to increase as the amount of the surfactants increased for both butter and pork lard samples, as shown in Fig. 2(e–h) and Fig. 3(e–
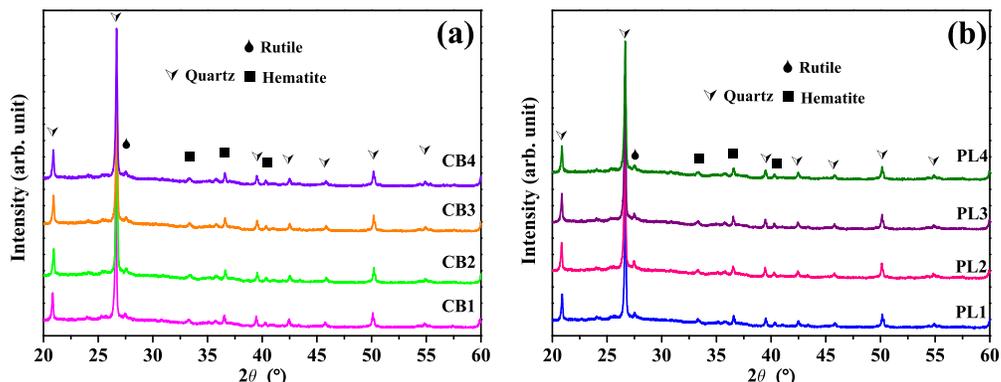
Fig. 1 X-ray diffraction patterns of PAS samples: (a) cow butter as a surfactant and (b) pork lard as a surfactant.
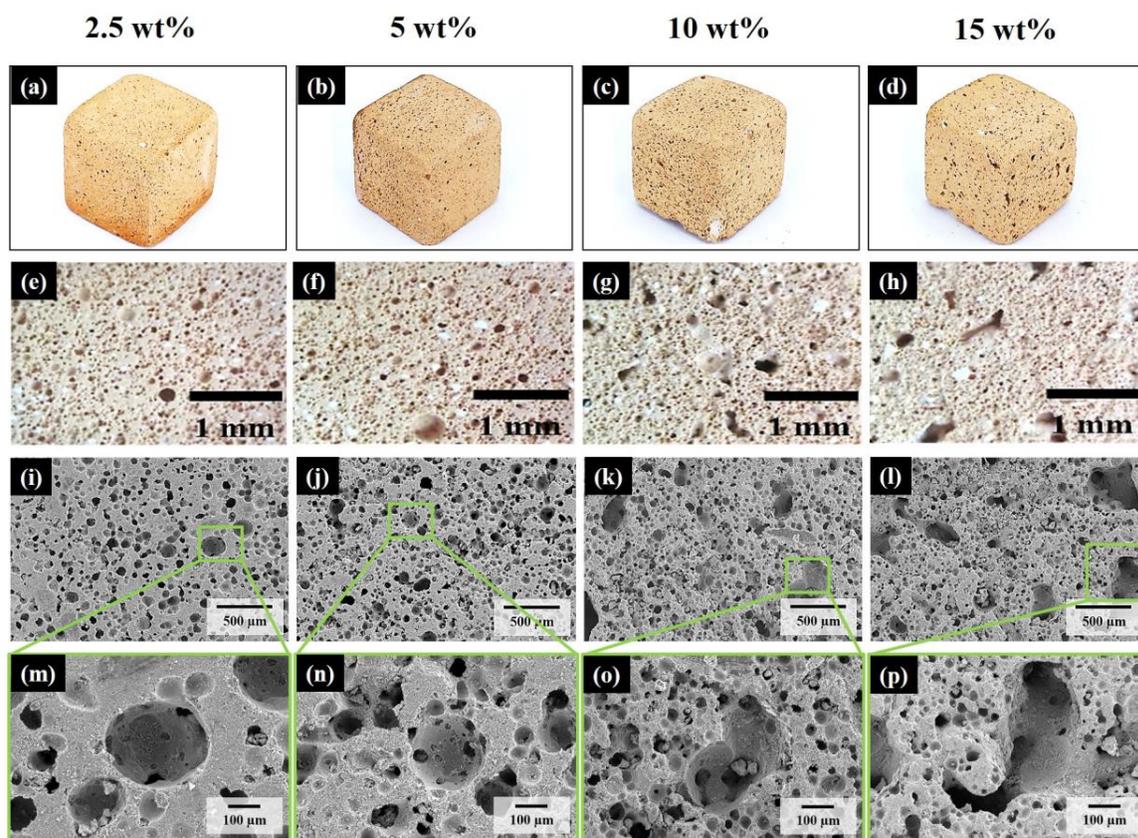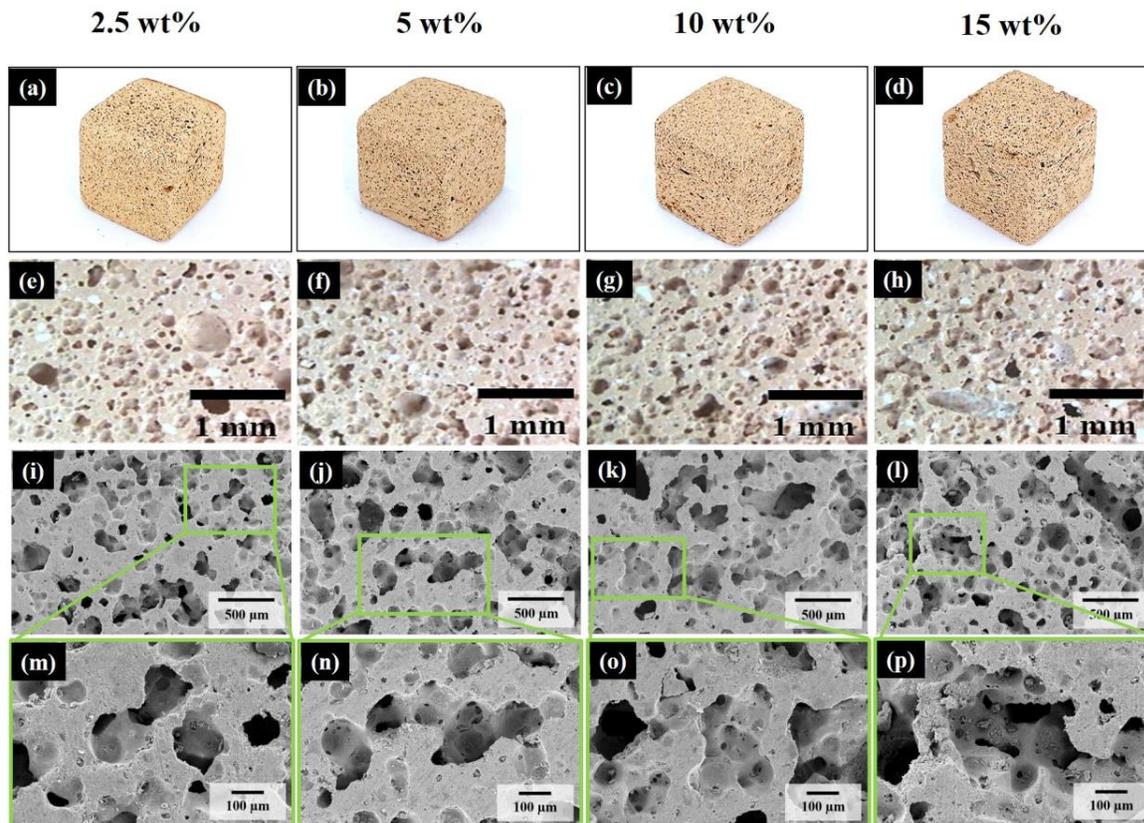

Fig. 2 (a–d) The prototype precasts of PAS samples, (e–h) optical images, (i–l) SEM micrographs, and (m–p) closer examination of the SEM micrographs at selected areas for PAS samples with cow butter as a surfactant.

h), respectively.

The SEM images of PAS samples containing butter and pork lard are shown in Fig. 2(i–p) and Fig. 3(i–p), respectively. The type of surfactant used, with respect to butter and pork lard, was found to have an effect on the morphology of PAS samples which produced well interconnected pores

(open pores). Furthermore, the amount of open pores increased as amounts of surfactant increased. As shown in previous works, the morphology of geopolymer foam formed when H_2O_2 was used as a foaming agent normally gave large sphere-shaped pores [35]. That is due to H_2O_2 reacting with alkaline solutions to generate gas, which causes

Fig. 3 (a–d) The prototype precasts of PAS samples, (e–h) optical images, (i–l) SEM micrographs, and (m–p) closer examination of SEM micrographs at selected areas for PAS samples with pork lard as a surfactant.
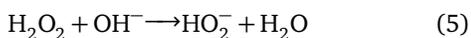
a porous microstructure in the samples [36, 37] because H_2O_2 decomposes to H_2O and O_2 according to the following equations [36]:

$$H_2O_2 + OH^- \longrightarrow HO_2^- + H_2O \qquad (5)$$

$$HO_2 + H_2O_2 \longrightarrow H_2O + O_2 + OH^- \qquad (6)$$
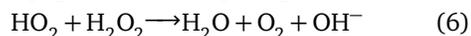
In the present work, the PAS samples that combined H_2O_2 as a foaming agent and butter as a surfactant exhibited morphology having a shape similar to what was found in a previous work [24], in agreement with published literature [16, 24]. On the other hand, the morphology of pork lard PAS samples exhibited distorted spherical or oblong shapes.

The values of bulk density and total porosity (p) of PAS samples are shown in Table 3. It was found that the pork lard PAS samples exhibited higher values of density than the butter PAS samples. When the amount of surfactant increased, the density value decreased from 0.85–0.71 g/cm³ and from 0.87–0.75 g/cm³ for butter and pork lard (2.5–15

Table 3 Bulk density and total porosity of PAS samples as a function of the amount of surfactant.

Sample	H_2O_2 (wt%)	Surfactant (wt%)		Bulk density (g/cm³)	Total porosity (%)
		Butter	Pork lard		
GCB1	2.4	2.5	–	0.85 ± 0.02	62.5 ± 0.3
GCB2	2.4	5	–	0.80 ± 0.03	64.5 ± 0.5
GCB3	2.4	10	–	0.72 ± 0.01	67.4 ± 0.2
GCB4	2.4	15	–	0.71 ± 0.01	67.8 ± 0.1
GPL1	2.4	–	2	0.87 ± 0.02	59.3 ± 0.4
GPL2	2.4	–	5	0.86 ± 0.01	61.2 ± 0.1
GPL3	2.4	–	10	0.79 ± 0.03	65.4 ± 0.3
GPL4	2.4	–	15	0.75 ± 0.02	66.9 ± 0.3

wt% samples), respectively. This may be due to the morphology of the pores having agglomerated together to become larger pores at a high amount of surfactant (Fig. 2 and Fig. 3). Fig. 4 shows the values of porosity and water absorption for PAS samples having different amounts of butter and pork lard. Both porosity and water absorption increased as the amount of surfactant increased, which corresponded to the decreases of density
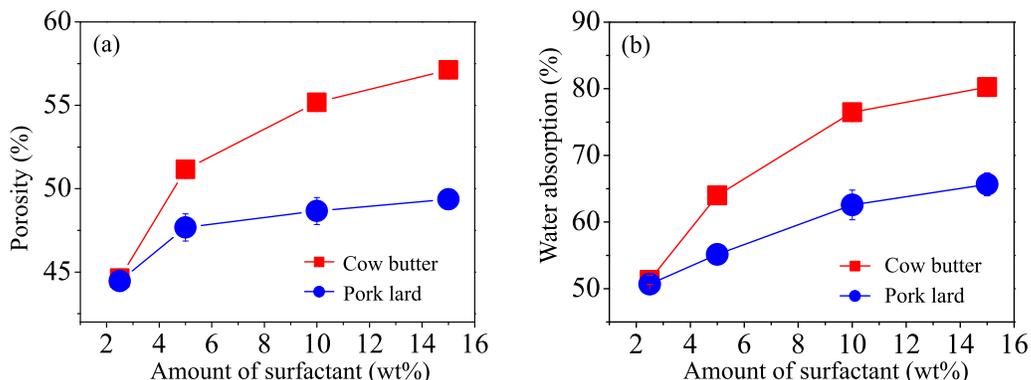
Fig. 4 (a) Porosity and (b) water absorption of PAS samples with varying amounts of surfactant.
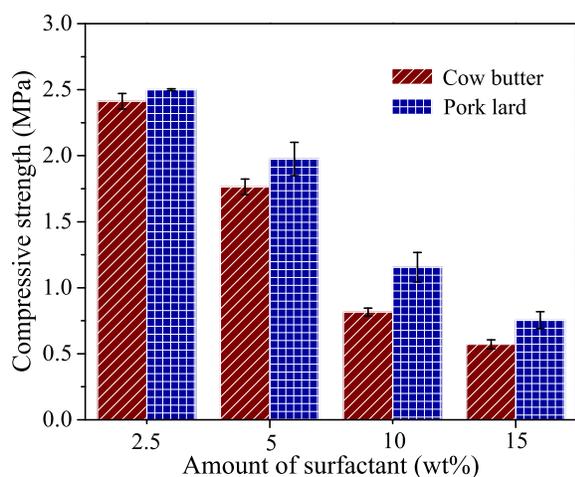

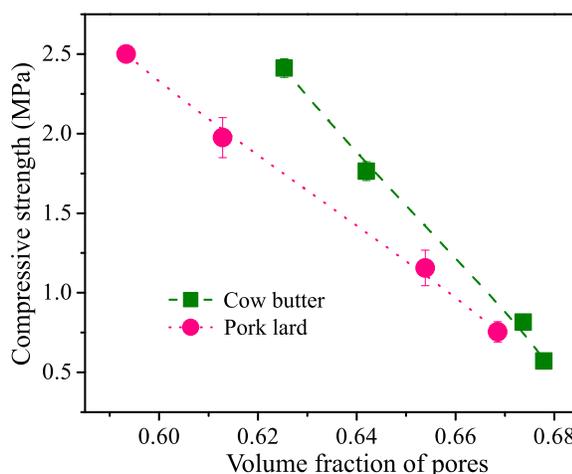**Fig. 5** Compressive strength of PAS samples with varying amounts of surfactant.

Fig. 6 The plot of compressive strength versus volume fraction of pores for PAS samples.

value (Table 3). The porosity value increased from 45.16–49.36% and from 43.14–57.12% for butter and pork lard, respectively. In the same direction, the water absorption value increased from 50.51–80.26% and 51.88–65.66% (2.5–15 wt% samples), for butter and pork lard, respectively. The butter PAS samples may have had higher porosity and water absorption values at the same amount of surfactant as the pork lard PAS samples because of the different lather properties of the surfactants due to the composition of aliphatic chains producing different types of soap molecules [24, 26]. Normally, the reaction between oil and a strong alkaline solution produces *in situ* carboxylate surfactants (soap molecules) via the saponification reaction, which consists of the hydrolysis of the triglycerides (found in oil or fats), plus glyceride, and glycerol (a water-soluble molecule) [25].

The compressive strengths of PAS samples are shown in Fig. 5. The compressive strength value decreased when the surfactant content increased. However, the pork lard PAS samples exhibited higher compressive strength than the butter PAS samples, agreeing with the porosity results in which high amounts of porosity decreased compressive strength. Normally, the relationship between strength and total porosity (Table 3) can be explained by several models. However, a simple equation (7) proposed by Ryshkewitch [38] describes the strength (σ) of a porous material related to total porosity (p) [21]:

$$\sigma = \sigma_0 \, e^{bp} \qquad (7)$$

where σ is the strength of a material at relative total porosity p, σ_0 is a constant, and b is a parameter determined by pore characteristics. The strength

and total porosity values data (Fig. 5 and Table 3) were well fitted by the equation (7) as shown in Fig. 6. The *b* values for butter and pork lard samples were 25.97 (with a correlation factor $R^2 = 0.95$) and 15.18 ($R^2 = 0.96$), respectively. This result is consistent with previous works on porous ceramics [16, 24, 39, 40].

CONCLUSION

In this work, the porous alumino-siliceous materials were successfully synthesized by geopolymerization using H_2O_2 as a foaming agent with different surfactants (butter or pork lard). The type of surfactant used, with respect to butter or pork lard, was found to have an effect on the morphology of the PAS samples, and they produced the open pores. The PAS samples were characterized by large sphere-shaped pores when butter was used, and distorted spherical or oblong shaped pores when pork lard was used. This result is due to the lather properties of the different surfactants, and therefore producing different types of soap molecules. The butter provided the best combination, in terms of porosity and water absorption values. The trend of compressive strength was related to porosity, a high amount of pork lard decreased the compressive strength. The relationship between the porosity and strength can be described by the Ryshkewitch model. The PAS materials with animal oil and animal products have a potential for using as highly porous material with wide applications.

REFERENCES

1. Bediako M (2018) Pozzolanic potentials and hydration behavior of ground waste clay brick obtained from clamp-firing technology. *Case Stud Constr Mater* **8**, 1–7.
2. Fernandez R, Martirena F, Scrivener KL (2011) The origin of the pozzolanic activity of calcined clay minerals: A comparison between kaolinite, illite and montmorillonite. *Cem Concr Res* **41**, 113–122.
3. Seraj S, Ferron RD, Juenger MCG (2016) Calcining natural zeolites to improve their effect on cementitious mixture workability. *Cem Concr Res* **85**, 102–110.
4. Nikolov A, Rostovsky I, Nugteren H (2017) Geopolymer materials based on natural zeolite. *Case Stud Constr Mater* **6**, 198–205.
5. Abdel-Ghani NT, Elsayed HA, Abdel-Moied S (2018) Geopolymer synthesis by the alkali-activation of blastfurnace steel slag and its fire-resistance. *HBRC J* **14**, 159–164.
6. Alehyen S, Achouri ME, Taibi M (2017) Characterization, microstructure and properties of fly ash-based geopolymer. *J Mater Environ Sci* **8**, 1783–1796.
7. Davidovits J (1988) Geopolymers of the first generation: siliface-process, geopolymer. *Geopolymer* **88**, 49–67.
8. Lin L, Wang S, Zhu Z (2006) Main factors affecting mechanical characteristics of geopolymer revealed by experimental design and associated statistical analysis. *J Colloid Interface Sci* **300**, 52–59.
9. Huang Y, Han M (2011) The influence of Al_2O_3 addition on microstructure, mechanical and formaldehyde adsorption properties of fly ash-based geopolymer products. *J Hazard Mater* **193**, 90–94.
10. He P, Jia D, Wang S (2013) Microstructure and integrity of leucite ceramic derived from potassium-based geopolymer precursor. *J Eur Ceram Soc* **33**, 689–698.
11. Schmücker M, MacKenzie KJD (2005) Microstructure of sodium polysialate siloxo geopolymer. *Ceram Int* **31**, 433–437.
12. Duxson P, Lukey GC, Deventer JSJ (2007) Physical evolution of Na-geopolymer derived from metakaolin up to 1000 °C. *J Mater Sci* **42**, 3044–3054.
13. Ferone C, Roviello G, Colangelo F, Cioffi R, Tarallo O (2013) Novel hybrid organic-geopolymer materials. *App Clay Sci* **73**, 42–50.
14. Zhang Z, Provis JL, Reid A, Wang H (2014) Geopolymer foam concrete: An emerging material for sustainable construction. *Constr Build Mater* **56**, 113–127.
15. Verdolotti L, Liguori B, Capasso I, Errico A, Caputo D, Lavorgna M, Iannace S (2015) Synergistic effect of vegetable protein and silicon addition on geopolymeric foams properties. *J Mater Sci* **50**, 2459–2466.
16. Bai C, Franchin G, Elsayed H, Conte A, Colombo P (2016) High strength metakaolin-based geopolymer foams with variable macro-porous structure. *J Eur Ceram Soc* **36**, 4243–4249.
17. Škvára F, Šulc R, Tišler Z, Skřičík P, šmilauer V, Cílová ZZ (2014) Preparation and properties of fly ash-based geopolymer foams. *Ceram Silikaty* **58**, 188–197.
18. Prud'homme E, Michaud P, Joussein E, Peyratout C, Smith A, Arrii-Clacens S, Clacens JM, Rossignol S (2010) Silica fume as porogent agent in geomaterials at low temperature. *J Eur Ceram Soc* **30**, 1641–1648.

19. Ducman V, Korat L (2016) Characterization of geopolymer fly-ash based foams obtained with the addition of Al powder or H_2O_2 as foaming agents. *Mater Charact* **113**, 207–213.

20. Bai C, Franchin G, Elsayed H, Zaggia A, Conte L, Li H, Colombo P (2017) High-porosity geopolymer foams with tailored porosity for thermal insulation and wastewater treatment. *J Mater Res* **32**, 3251–3259.

21. Bai C, Colombo P (2018) Processing, properties and applications of highly porous geopolymers: A review. *Ceram Int* **44**, 16103–16118.

22. Yun-Ming L, Cheng-Yong H, Mustafa M, Bakri A, Hussin K (2016) Structure and properties of clay based geopolymer cements: A review. *Prog Mater Sci* **83**, 595–629.

23. Bai C, Colombo P (2017) High-porosity geopolymer membrane supports by peroxide route with the addition of egg white as surfactant. *Ceram Int* **43**, 2267–2273.

24. Bai C, Ni T, Wang Q, Li H, Colombo P (2018) Porosity, mechanical and insulating properties of geopolymer foams using vegetable oil as the stabilizing agent. *J Eur Ceram Soc* **38**, 799–805.

25. Cilla MS, Morelli MR, Colombo P (2014) Open cell geopolymer foams by a novel saponification/peroxide/gelcasting combined route. *J Eur Ceram Soc* **34**, 3133–3137.

26. Cilla MS, Innocentini MDM, Morelli MR, Colombo P (2017) Geopolymer foams obtained by the saponification/peroxide/gelcasting combined route using different soap foam precursors. *J Am Ceram Soc* **100**, 3440–3450.

27. Anneken DJ, Both S, Christoph R, Fieg G, Steinberner U, Westfechtel A (2006) Fatty acids. In: *Ullmann's Encyclopedia of Industrial Chemistry*, Wiley-VCH, Germany.

28. Bockisch M (1998) *Fats and Oils Handbook*, AOCS Press, MA, USA.

29. Gunstone FD (2004) *The Chemistry of Oils and Fats: Sources Composition Properties and Uses*, Blackwell Publishing Ltd., NJ, USA.

30. Shahidi F (2005) *Bailey's Industrial Oil and Fat Products*, Wiley-Interscience, NJ, USA.

31. Toscano G, Riva G, Foppa Pedretti E, Duca D (2012) Vegetable oil and fat viscosity forecast models based on iodine number and saponification number. *Biomass Bioenerg* **46**, 511–516.

32. Silva RC, Cotting LN, Poltronieri TP, Balcão VM, Gioielli LA (2009) Physical properties of structured lipids from lard and soybean oil produced by enzymatic interesterification. *Ciênc Tecnol Aliment Campinas* **29**, 652–660.

33. Rohman A, Triyana K, Sismindari Y, Erwanto Y (2012) Differentiation of lard and other animal fats based on triacylglycerols composition and principal component analysis. *Int Food Res J* **19**, 475–479.

34. Azouz A (2011) Nutritional evaluation of children Egyptian school meal: I – Fat sources and fatty acids profile. *Ann Agric Sci* **56**, 73–76.

35. Kaewapai K, Lertcumfu N, Jaita P, Manotham S, Tunkasiri T, Malasri P, Rujijanagul G (2019) Preparation and characterization of ceramic waste-based geopolymer ceramic composites for substrate culture application. *Key Eng Mater* **798**, 194–199.

36. Masia G, Rickard WDA, Vickers L, Bignozzi MC, Riessen A (2014) A comparison between different foaming methods for the synthesis of light weight geopolymers. *Ceram Int* **40**, 13891–13902.

37. Zhang Z, Provis JL, Reid A, Wang H (2014) Geopolymer foam concrete: An emerging material for sustainable construction. *Constr Build Mater* **56**, 113–127.

38. Ryshkewitch E (1953) Compression strength of porous sintered alumina and zirconia. *J Am Ceram Soc* **36**, 65–68.

39. Bai C, Deng X, Li J, Jing Y, Jiang W (2014) Preparation and properties of mullite-bonded porous SiC ceramics using porous alumina as oxide. *Mater Charact* **90**, 81–87.

40. Li J, Lin H, Li J (2011) Factors that influence the flexural strength of SiC-based porous ceramics used for hot gas filter support. *J Eur Ceram Soc* **31**, 825–831.